

# *Commissioning and First Data Analysis of the Mainz Radius Experiment*

Adriano Del Vincio 562946

Relatori: prof. Francesco Forti, Prof. Concettina Sfienti

Università di Pisa

20/07/2023



UNIVERSITÀ DI PISA

# The Mainz Radius Experiment

MREX

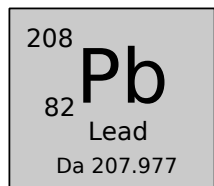
The Mainz Radius Experiment is an experimental campaign at the nuclear physics institute of Mainz, with the aim of investigating the properties of nuclear matter with imbalance in the number of protons and neutrons.

## Objective

Determination of the neutron spacial density for  $^{208}Pb$  nucleus, through the elastic electron scattering. From an accurate determination of the neutron spacial distribution, the *Neutron Skin Thickness* of  $^{208}Pb$  is measured.

The neutron skin thickness is defined as the difference between rms radius of neutron and proton spacial distributions:

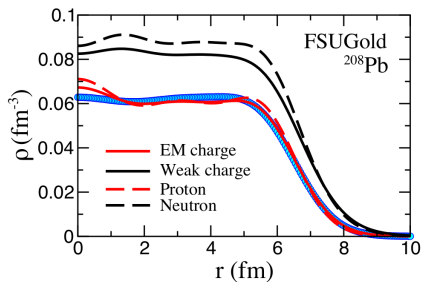
$$\delta r_{np} = \sqrt{\langle r_n^2 \rangle} - \sqrt{\langle r_p^2 \rangle}, \quad (1)$$



## MREX and Neutron Skin Thickness

The results of the experiment will be valuable to constrain the Equation of State (**EOS**) of nuclear matter. The EOS of nuclear matter plays an important role for the **neutron star structure**, specifically the determination of the radius  $R_{ns}$ .

In neutron rich nuclei, the spacial distribution of neutrons is **more extended** than proton one. Theoretical models link the Neutron skin thickness of heavy nuclei, such as  $^{208}Pb$ , with the slope of the symmetry energy **L**.

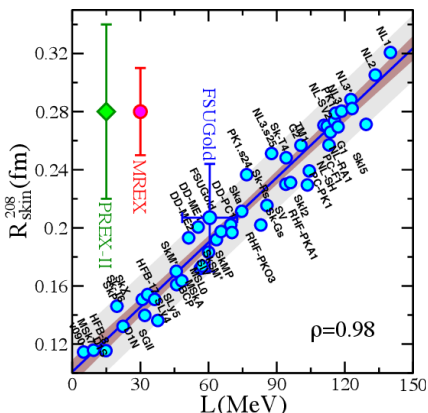


Neutron (black line) and proton (red line) spacial distributions as predicted by FSUGold model. The blue dots represents the experimental data of  $^{208}Pb$  charge density.

# Symmetry Energy

## Neutron Skin and Symmetry Energy

$$\epsilon(\rho, \alpha) = \epsilon_{SNM}(\rho) + \alpha^2 S(\rho) + O(\alpha^4)$$
$$S(\rho) = J + L \cdot \left( \frac{\rho - \rho_0}{3\rho_0} \right) + \dots \quad (2)$$

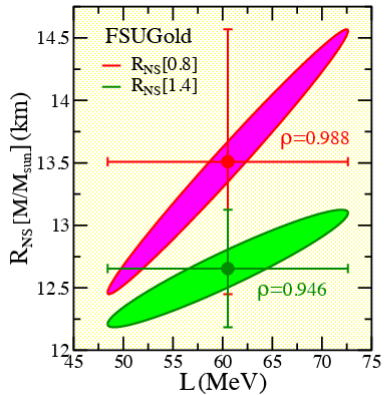


The symmetry energy  $S(\rho)$  is the key component of the equation of state which controls the neutron skin thickness.  $S(\rho)$  quantifies the change in energy related to the neutron-proton asymmetry.

## Neutron Skin and Neutron Star Radius

The slope of the symmetry energy is related to both the **neutron skin** of lead and **neutron star radius**. The radius of the neutron star is determined from Tolman-Oppenheimer-Volkoff (TOV) equation. Giving the pressure  $P_c$  at the center of the star, the radius  $R$  can be determined. But for neutron star, the pressure at the center is strongly related to the **pressure of pure neutron matter**, in large part determined by  $L$ .

$$P = \frac{1}{3} \rho_0 L \quad (3)$$



Covariance ellipses displaying the correlation between the neutron star radius and the slope of the symmetry energy, as predicted by FSUGold model.

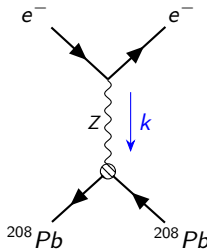
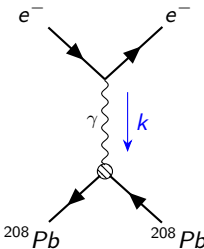
# Parity Violating Asymmetry

## Measurement of the Neutron Spacial Distribution of Lead

The determination of the neutron spacial distribution relies on the electron-nucleus elastic scattering. The neutron spacial distribution is measured via the parity violating scattering, where longitudinal polarized electrons scatter from a fixed lead target. The experiment is planned at the future MESA accelerator.

$$A_{pv} = \frac{\sigma_R - \sigma_L}{\sigma_R + \sigma_L} \quad (4)$$

The key quantity is the asymmetry in the cross-section due to the different polarization state of the beam.



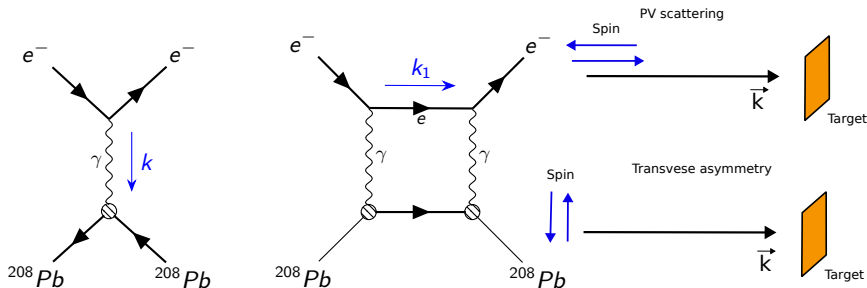
- $Q_p = 0.04$
- $Q_n = -0.99$

## Transverse Asymmetry

The transverse asymmetry, or Beam Normal Single Spin Asymmetry, is the cross-section asymmetry for electrons polarized in the normal plane ( $\frac{\vec{k}' \wedge \vec{k}}{|\vec{k}||\vec{k}'|}$ ) :

$$A_{transverse} = \frac{\sigma_{\uparrow} - \sigma_{\downarrow}}{\sigma_{\uparrow} + \sigma_{\downarrow}}$$

The asymmetry arises from the interference of:



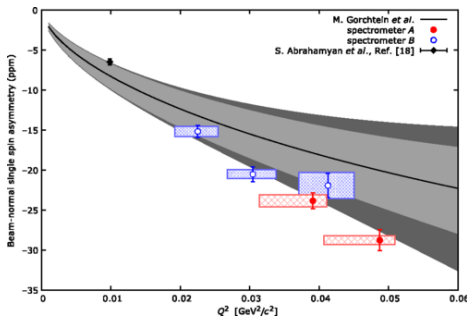
## Transverse Asymmetry

The incident beam is made by 570 MeV electrons, that are polarized along the transverse axes ( $\uparrow$  and  $\downarrow$ ). The physical quantity to measure is the asymmetry between the number of scattered electrons, due to the change of the polarity:

$$asym = \frac{N_+ - N_-}{N_+ + N_-} \text{ (expected } \sim +/- 20 \text{ ppm, } Q = 0.2 \text{ GeVc}^{-1}) \quad (5)$$

The prediction for the transverse asymmetry is given by the formula below:

$$A_n \simeq C_0 \log \frac{Q^2}{m_e^2 c^2} \frac{F_{Compton}(Q^2)}{F_{ch}(Q^2)} \quad (6)$$

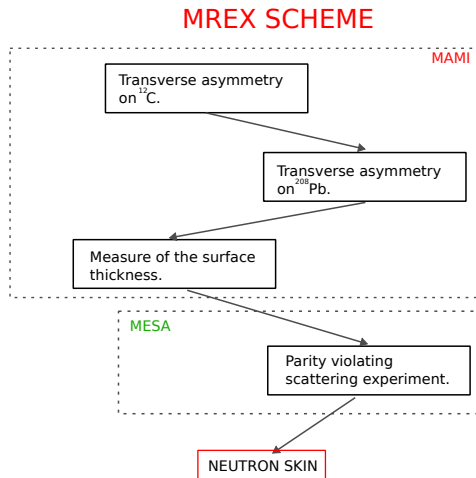


Asymmetry versus transferred momentum for selected nuclei.

# MREX SCHEME

Scheme of the experimental campaign of MREX. The work of the thesis correspond to the first step of the diagram, the commissioning of the new setup for the measurement of the transverse asymmetry on  $^{12}\text{C}$ .

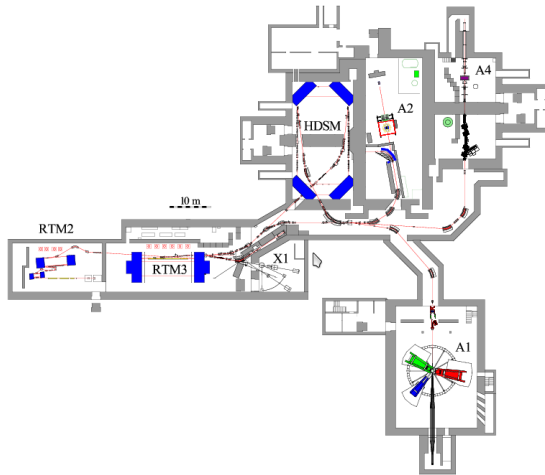
- Detector test in the laboratory.
- Development of the analysis program.
- Calibration of the Beam monitor to measure the beam parameters.
- Data analysis and extraction of the transverse asymmetry on  $^{12}\text{C}$ .
- Measurement of the rates with lead target.



Scheme of MREX.

# MAMI ELECTRON ACCELERATOR

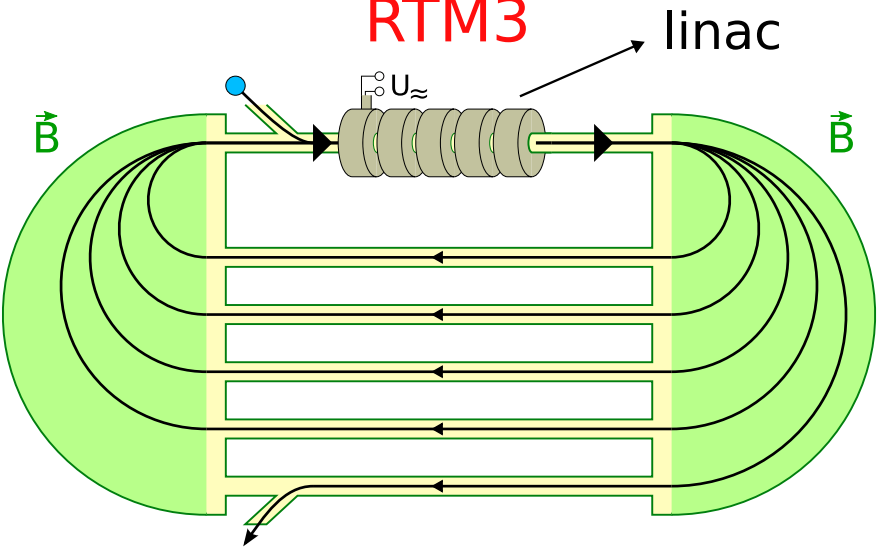
# MAMI Electron Accelerator



Scheme of MAMI accelerator. RTM2 is the first acceleration stage, where the electrons are extracted from the source. RTM3 corresponds to the final acceleration stage of the experiment (570 MeV), A1 is the experiment hall where the experiment described is the thesis is set up.

## Race Track Microtron Scheme

RTM3



# RTM3

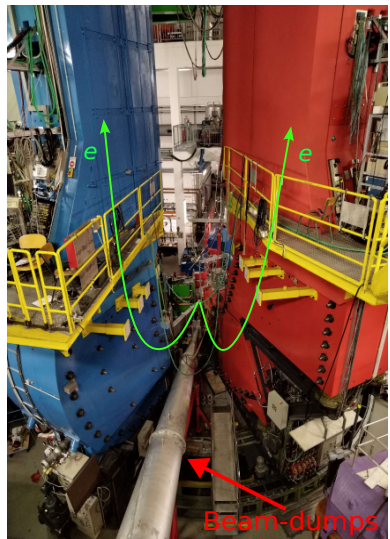
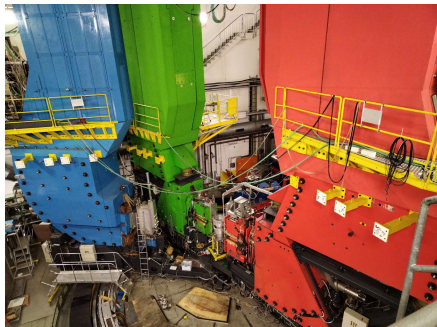
Race Track Microtron 3 of MAMI



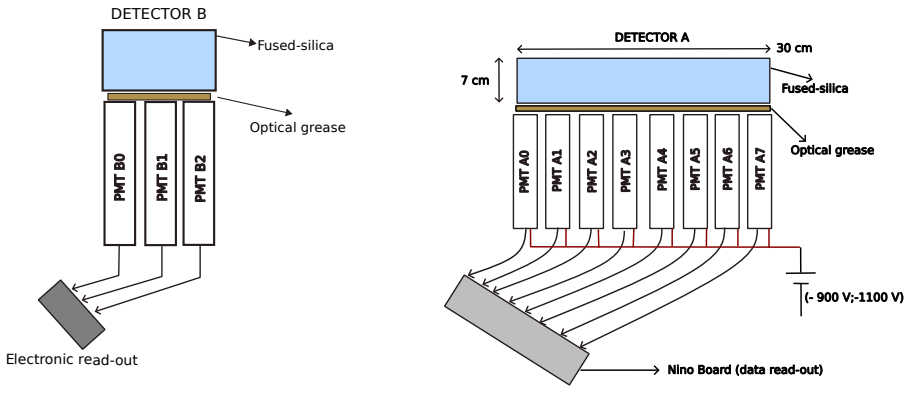
# A1 Experimental Hall

## MAMI Electron Accelerator

In MAMI A1, three large spectrometers are positioned on a rail track around the scattering chamber. For the experiment, only the red and blue spectrometers were used.



# Cherenkov Detectors



Scheme of detector B (on the left) and detector A (on the right).

# NINO Asic Board

## Data Acquisition Electronics

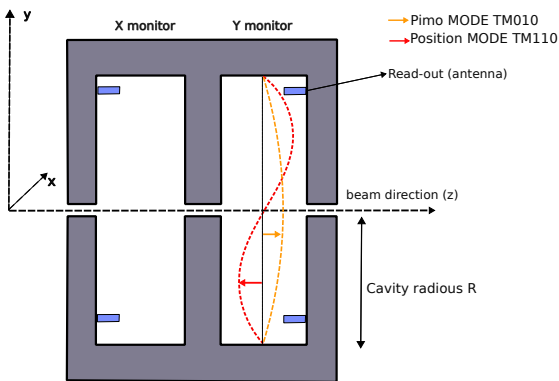
The NINO board is the DAQ system that counts the input signals coming from the Cherenkov detectors.

- 32 input channels.
- Attenuation circuit for each input channel.
- Common current threshold for 4 adjacent channels.



# MAMI Beam Monitors

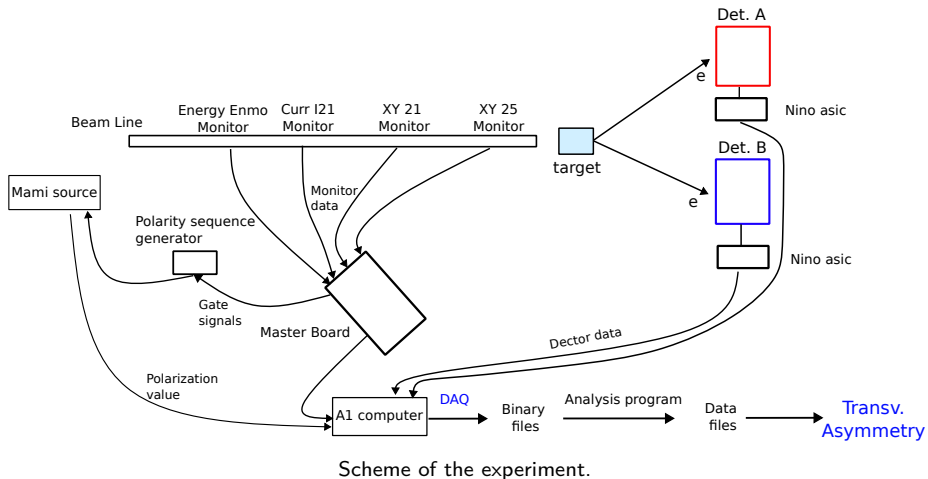
At MAMI the beam parameters, as **X,Y** transverse positions, **Energy** and **Current** are measured by resonant cavities.



Accurate calibration of the cavities voltage output performed as part of the analysis. The beam parameters are measured to take care of possible false asymmetries that arises from the variations of the beam parameters.

Scheme of the resonant cavity in MAMI, with the different electromagnetic modes excited by the beam passage.

# General Scheme of the Experiment



## BEAM TIME AND CALIBRATIONS

## Beam-time 29/11/2022 - 5/12/2022

### Beam Normal Single Spin Asymmetry at MAMI

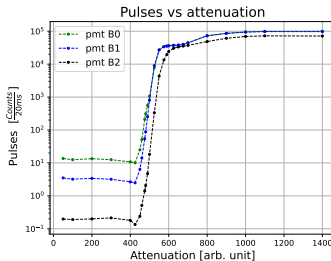
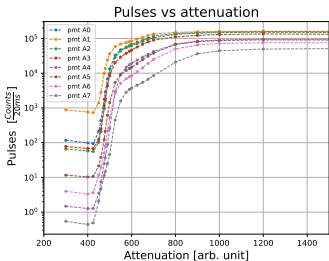
During the last beam-time, several measurements were performed at Mainz Mikrotron MAMI. The last data acquisition campaign had the following goals:

- Test the new **data acquisition system**, developed for the new setup with a low rate signals ( $\simeq 1$  MHz).
- Measure the **transverse asymmetry**  $A_n$  of  $^{12}C$ .
- Measure the expected **rates** on  $^{208}Pb$  target, in anticipation of the future measurement of  $A_n$  for lead.
- Long term goal: acquire more knowledge on the **systematic effects** that the transverse asymmetry has on the measurement of the Parity-violating asymmetry.

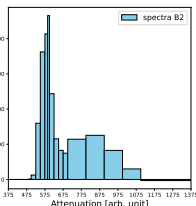
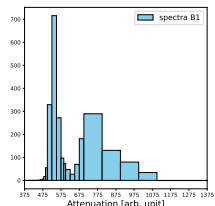
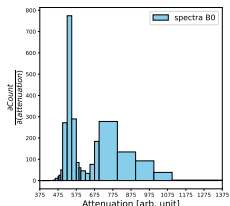
Variation of the beam parameters can influence the measurements, inducing false asymmetries. These effects are corrected during the analysis.

# PMTs Signal Optimization

## Adjustament of threshold



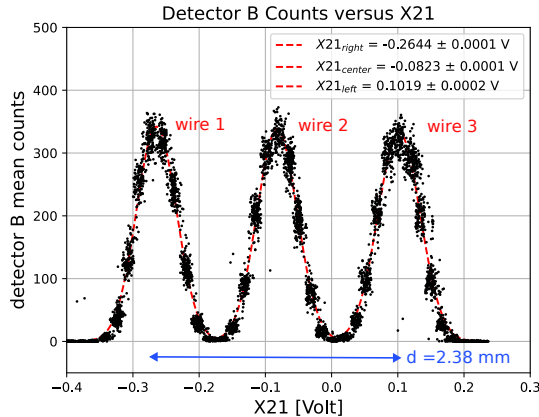
Counts versus attenuation value for PMTs of detector A (left plot) and B (right plot).



# Calibration of the Beam Monitors

## Beam Position (X,Y) on the target

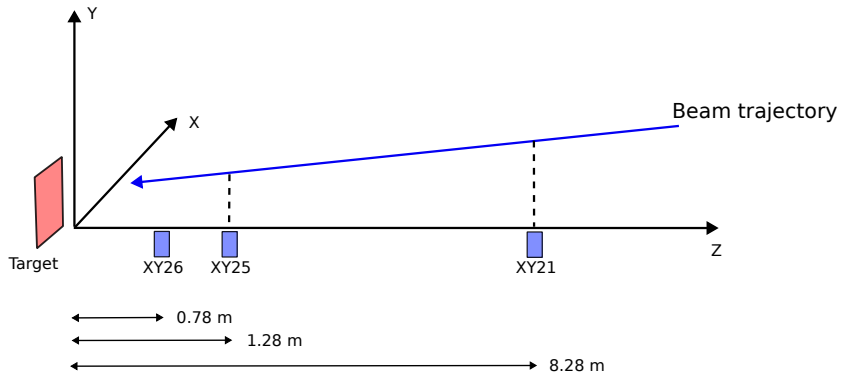
Calibrate XY measurement by inserting a dedicated target with scattering wires at known distance and moving the beam across the target.



Calibration of the X21 monitor.

# Calibration of the Beam Monitors

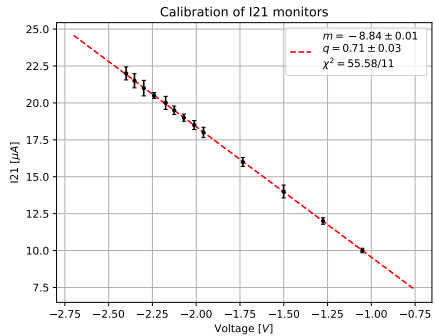
Beam Position ( $X, Y$ ) on the target



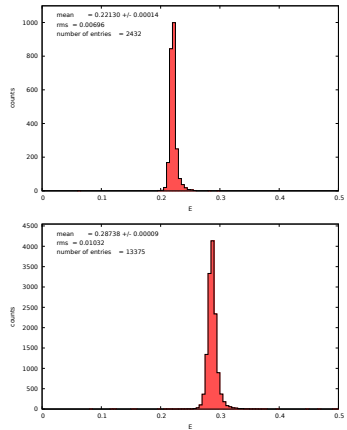
The beam is assumed following a straight path given by  $x, y = m \cdot z + q_{x,y}$ , the  $(X, Y)$  coordinates are given by  $q_{x,y}$

# Beam Energy and Beam Current

The conversion parameters from V to  $\mu\text{A}$  and keV are measured with scans in current and energy around the nominal values.



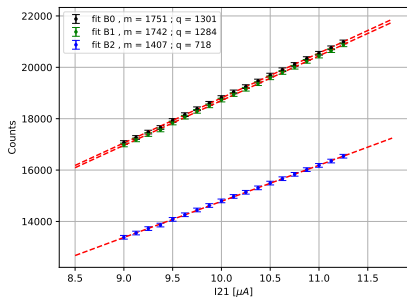
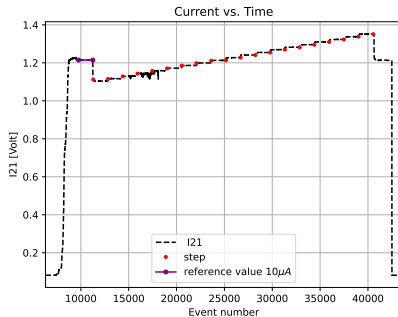
Current monitor I21. On the x axis the voltage signal of the PIMO monitor, on the y axis the nominal current of the beam.



Calibration of the energy monitor. For the first histogram the current is 15  $\mu\text{A}$ , 20  $\mu\text{A}$  for the second one.

## Auto-Calibration procedure

Every 3 hours of beam, a special operation mode of MAMI is set. The current is raised in small steps, from  $9 \mu\text{A}$  to  $11.125 \mu\text{A}$ . This is used to check the linearity of the PMTs through time, and to measure the PMT offset, that is subtracted later from the data.

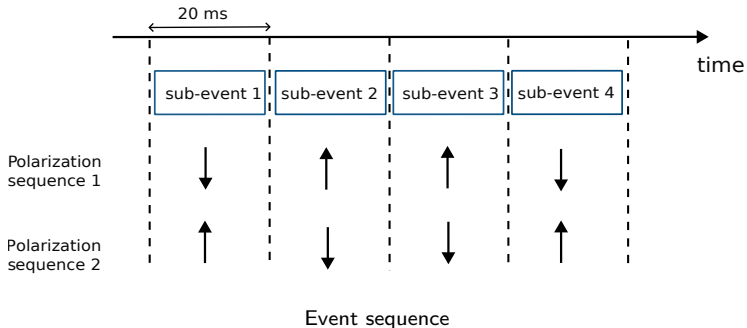


## DATA ANALYSIS

## Structure of the event

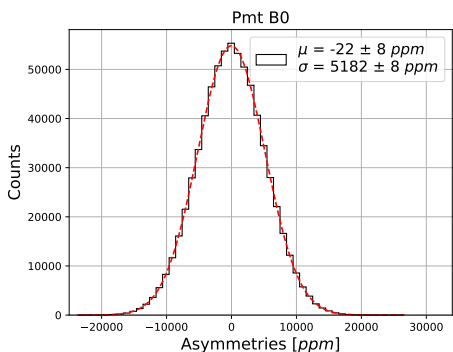
$$A_{mes.} = \frac{(N_1 + N_4) - (N_2 + N_3)}{(N_1 + N_4) + (N_2 + N_3)} \quad (7)$$

The Data are divided in a series of events (80 ms), that correspond to 4 sequential sub-event. For each sub-event there is a precise polarization of the Beam. During the 20 ms of the sub-event, all the electrons are counted.



## Analysis on Carbon Target

Each event corresponds to a single measurement of the asymmetry  $A$ . With this experiment, an amount of 1 million events have been collected. The asymmetry data are normally distributed:



$$\begin{aligned} \text{Var}[A_{\text{asym}}] &= \text{Var}\left[\frac{N_{\uparrow} - N_{\downarrow}}{N_{\uparrow} + N_{\downarrow}}\right] \simeq \frac{\text{Var}[N_{\uparrow} - N_{\downarrow}]}{(N_{\uparrow} + N_{\downarrow})^2} \\ \frac{2\text{Var}[N]}{4N^2} &= \frac{1}{2N} \quad \sigma = \frac{1}{\sqrt{2N}} \end{aligned}$$

Where it is supposed that the PMTs counts are normal distributed, with  $\mu$  equal to  $\sigma^2$ . The rms associated to the sample mean decreases as the  $\sqrt{N_{\text{measure}}}$ . With the statistical error is:

$$\sigma = \frac{1}{\sqrt{2N \cdot N_{\text{measure}}}} \quad (8)$$

Considering  $6.5 \cdot 10^5$  events and  $\mu = 20000$  counts per PMT (similar to what was measured for PMT B0):

- $\sigma = 8 \text{ ppm}$ .

## Model For Fitting the Data

Considering that  $A$  for  $^{12}C$  is expected to be  $\simeq 20\text{ ppm}$ , small fluctuations of the beam correlated to the polarization can produce false asymmetries. The important parameters are:

- **X, Y** positions of the beam spot on the target.
- beam current **I**.
- beam energy **E**.
- incident angles of the beam  $\theta_x, \theta_y$

The final model uses a **linear expansion** on the beam parameters, since the variations are small:

$$A_{tot} = A_{physical} \cdot P + \delta_I + A_x \delta x + A_y \delta y + A_{\theta_x} \delta \theta_x + A_{\theta_y} \delta \theta_y + A_E \delta E \quad (9)$$

Each  $\delta q$  is computed as the mean difference between up and down polarized sub-events:

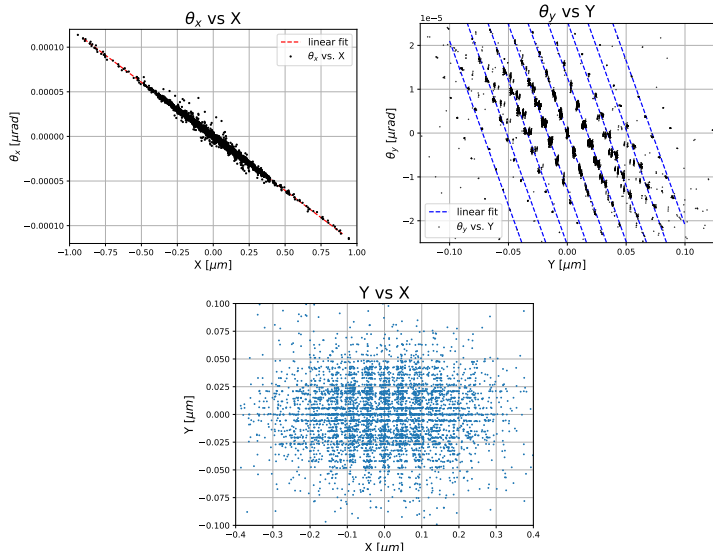
$$\delta q = \frac{q_{\uparrow,0} + q_{\uparrow,1}}{2} - \frac{q_{\downarrow,0} + q_{\downarrow,1}}{2} \quad (10)$$

The current asymmetry is defined differently. Because the scattering rate is proportional to the beam current, the model contains the current asymmetry directly:

$$\delta I = \frac{I_{\uparrow} - I_{\downarrow}}{I_{\uparrow} + I_{\downarrow}} \quad (11)$$

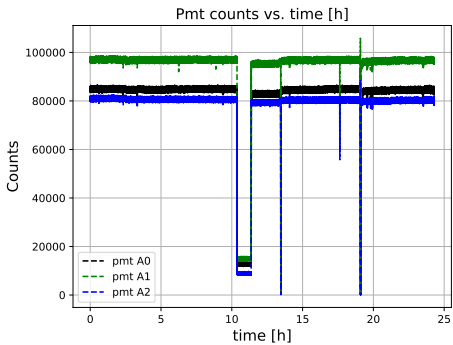
# Beam Parameters Correlation

Considering the correlations, the final parameters of the model are **I**, **X**, **Y** and **E**.

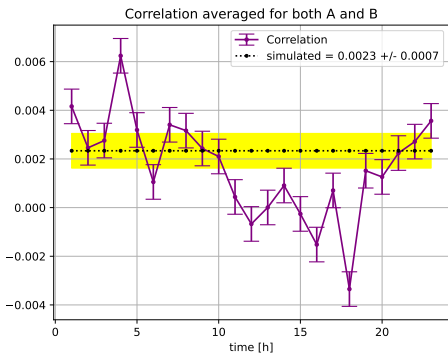


## Data Selection

Before proceeding in the analysis, an accurate data selection was performed, to remove the outliers, as well as data affected by anomalous variation of the beam current or polarization loss.



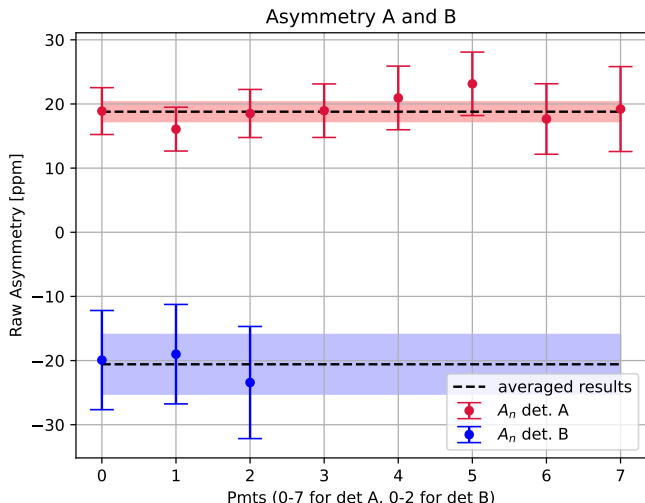
PMT counts of detector B versus time.



Correlation between the PMTs counts and the polarization. A loss of beam polarization can be identified at  $t = 11\text{ h}$ .

## Results

Final asymmetry result for each PMTs:



## Results

The result of the analysis is obtained combining the measured asymmetries for PMTs.

$$\bar{A} = \frac{\sum_i A_i \frac{1}{w_i}}{\frac{1}{w_i}} \quad w_i = \frac{1}{\sigma_i^2}$$

the final values of the Beam Normal Single Spin asymmetries are:

$$A_A = 23.1 \pm 1.7 \text{ ppm} \quad A_B = -21 \pm 5 \text{ ppm} \quad (12)$$

With a transfer momentum  $Q = 0.04 \text{ GeV}$ . Reversing the sign of the asymmetry for Det. B we notice that the two measurement are consistent within  $1\sigma$ . The values measured in this thesis work are in agreement with precedent measurement performed at MAMI, with the old electronic setup:

$$A_A = 23.9 \pm 1(\text{stat}) \pm 0.7(\text{syst}) \text{ ppm} \quad A_B = -21.9 \pm 1.5(\text{stat}) \pm 1.6(\text{syst}) \text{ ppm} \quad (13)$$

This demonstrates the validity of the new electronic setup that allows handling lower rates and paves the road to the future MREX measurements.

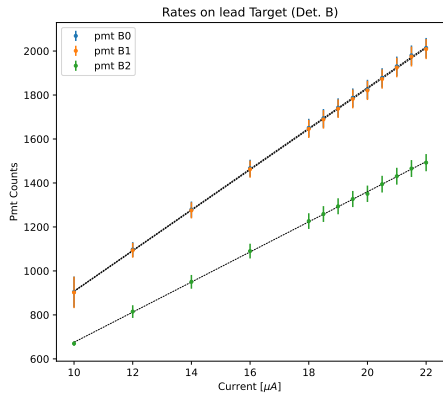
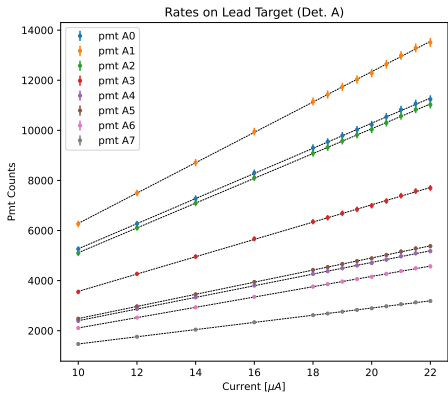
## Ringraziamenti

**GRAZIE A TUTTI PER L'ATTENZIONE**

## **ADDITIONAL MATERIAL**

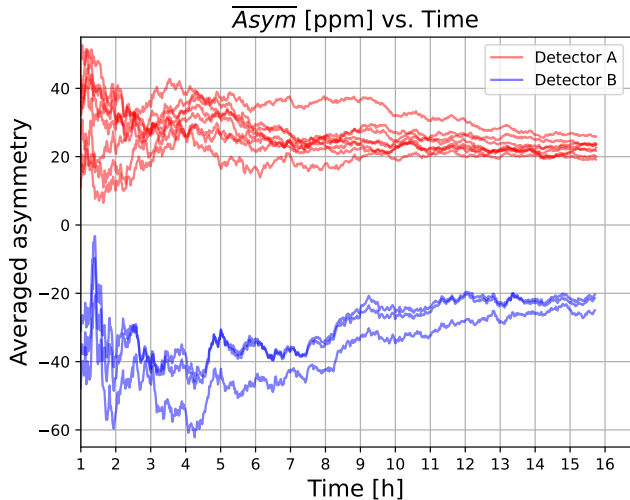
## Rates on Lead

The rates on lead target (1 mm thick) have been measured. The transverse asymmetry on lead will be the next step of MREX experiment. This measurement is mandatory to constrain the systematic error of PV experiment.



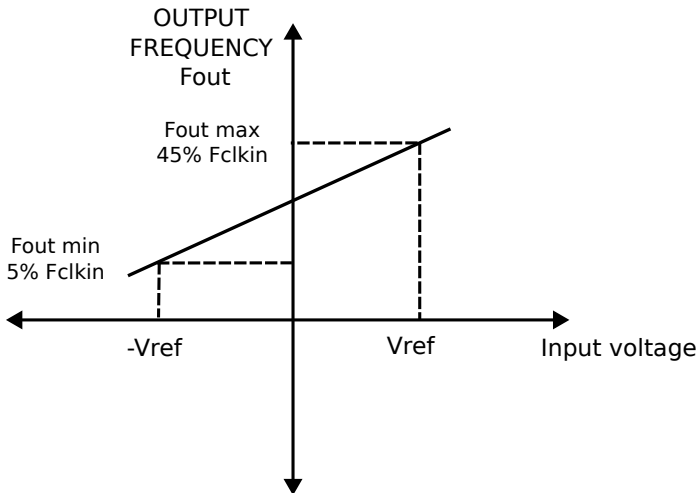
Since the rates are lower for lead compared to carbon, the statistics needed to measure  $A_n$  for  $^{208}Pb$  is 23 times the statistic accumulated for carbon.

Here a plot about the trend of the asymmetry as the data increases. The band is the error computed as showed in the previous slide, centered around the values of  $+20\text{ppm}$  for detector A and  $-20\text{ppm}$  for detector B.



## Voltage to Frequency Converters

The beam monitors are read-out with the voltage-to-frequency converters **VFC** devices, which produces an output signal whose frequency is proportional to the amplitude of the beam monitor signals.



## Description of the Process

The transverse asymmetry arises considering the time reversal operator. The time reversal operator reverses all the momenta and the spin direction.

